

Diagnosing quantum chaos with out-of-time-ordered-correlator quasiprobability in the kicked-top model

José Raúl González Alonso,¹ Nathan Shammah,^{2,3,4} Shahnawaz Ahmed,^{3,5} Franco Nori,^{3,6,7} and Justin Dressel^{1,8}

¹*Schmid College of Science and Technology, Chapman University, Orange, CA 92866, USA*

²*Unitary Fund*

³*Theoretical Quantum Physics Laboratory, RIKEN Cluster for Pioneering Research, Wako-shi, Saitama 351-0198, Japan*

⁴*Quantum Technology Lab, Dipartimento di Fisica, Università degli Studi di Milano, 20133 Milano, Italy*

⁵*Department of Microtechnology and Nanoscience, Applied Quantum Physics Laboratory, Chalmers University of Technology, Göteborg, Sweden.*

⁶*RIKEN Center for Quantum Computing (RQC), Wako-shi, Saitama 351-0198, Japan*

⁷*Department of Physics, University of Michigan, Ann Arbor, Michigan 48109-1040, USA*

⁸*Institute for Quantum Studies, Chapman University, Orange, CA 92866, USA*

(Dated: January 21, 2022)

While classical chaos has been successfully characterized with consistent theories and intuitive techniques, such as with the use of Lyapunov exponents, quantum chaos is still poorly understood, as well as its relation with multi-partite entanglement and information scrambling. We consider a benchmark system, the kicked top model, which displays chaotic behaviour in the classical version, and proceed to characterize the quantum case with a thorough diagnosis of the growth of chaos and entanglement in time. As a novel tool for the characterization of quantum chaos, we introduce for this scope the *quasi-probability distribution* behind the out-of-time-ordered correlator (OTOC). We calculate the cumulative nonclassicality of this distribution, which has already been shown to outperform the simple use of OTOC as a probe to distinguish between integrable and nonintegrable Hamiltonians. To provide a thorough comparative analysis, we contrast the behavior of the nonclassicality with entanglement measures, such as the tripartite mutual information of the Hamiltonian as well as the entanglement entropy. We find that systems whose initial states would lie in the “sea of chaos” in the classical kicked-top model, exhibit, as they evolve in time, characteristics associated with chaotic behavior and entanglement production in closed quantum systems. We corroborate this indication by capturing it with this novel OTOC-based measure.

I. INTRODUCTION

The concept of scrambling, initially introduced to characterize quantum chaos, has since been applied to quantum information processing, as it quantifies the delocalization of quantum information in a system. Out-of-time-ordered correlators (OTOCs) have been the subject of intense research as witnesses of scrambling, and as tools to study entanglement dynamics and quantum chaos [1–30]. However, a true understanding of the nature of quantum chaos and the limits of the usefulness of various diagnostic tools such as OTOCs to study chaos are the source of ongoing investigations both theoretically [31], and in recent experiments [32, 33].

As OTOCs measure time correlations among initially commuting operators, they provide a quantum counterpart to the classical and semiclassical theory of characterizing chaos using diverging trajectories with Lyapunov exponents.

While there have been indications of a connection between quantum chaos and scrambling, their mutual relationship needs to be fully elucidated, as well as their relationship with entanglement: for example, it has been shown that OTOCs can characterize chaotic dynamics in the quantum regime even where current entanglement witnesses saturate [27]. An analytical relationship between OTOCs and entanglement entropy, which is re-

lated to classical chaos quantifiers, has been shown in Ref. [34]. In the semiclassical regime this predicts the usual exponential growth for the OTOC and a linear growth of the entanglement entropy, characterized by the same Lyapunov exponent.

The cumulative nonclassicality of the quasi-probability distribution behind the out-of-time-ordered correlator exhibits different time scales that have been conjectured to be useful for distinguishing integrable and nonintegrable Hamiltonians [35]. That is, the time scales corresponding to regions where the quasi-probability distribution becomes negative or has a nonzero imaginary part can be used to identify behavior that cannot be explained classically. However, this conjecture was proposed in the context of spin chains with a notion of spatial locality [35].

In this work, we use the cumulative nonclassicality of the quasi-probability distribution to better characterize quantum information scrambling and quantum chaos in the quantum kicked top. Since this model contains second-momenta of collective angular momentum operators, which induce long-range interactions, it is a good candidate to study the interplay of quantum chaos and entanglement in a many-body quantum system. Moreover, since the simple kicked-top model has been extensively studied, e.g., the chaotic behavior is well understood in its classical counterpart, it represents a natural target to test and compare our novel analytical tool.

Additionally, we contrast the behavior of both the OTOC and the cumulative nonclassicality of its quasiprobability distribution with other measures used to diagnose scrambling and chaos. In particular, we study the von Neumann entropy of entanglement for a one to many partition of the system and the tripartite mutual information (TMI)[17, 36] of the unitary channel generated by the kicked-top Hamiltonian to elucidate the relationship between quantum chaos and scrambling in many-body systems that lack a notion of spatial locality.

We find that for small system sizes, all of the considered measures of quantum chaos and scrambling give poor, and even misleading, diagnostics. We provide an interpretation for these results, tailoring the standard notion of scrambling, based on the delocalization of information, to the case of the kicked-top, which lacks a notion of spatial locality.

This paper is organized as follows. We begin in Sec. II by presenting the model of a kicked-top that we use in our studies and present its classical phase space with chaotic features. In Sec. III A we motivate the study of OTOCs by using the square of the commutator between two operators. Then, in Sec. III, we introduce the various measures of quantum chaos and entanglement that we will compare: in Sec. III B we define the (coarse-grained) quasiprobability behind the OTOC and introduce a measure of nonclassicality based on it. In Sec. III C we present the tripartite mutual information definition for a channel and explain how it relates to a more general notion of scrambling. Our numerical results are shown in Sec. IV, where the various measures are compared both in time and in conjugate space, while the details of our calculations are presented in Appendix A. Finally, in Sec. V we present our conclusions and discuss future outlook of this work.

II. QUANTUM KICKED-TOP MODEL AND THE SEMICLASSICAL LIMIT

We are interested in studying the OTOC, and its coarse-grained quasiprobability distribution, for a system without a notion of spatial locality and that can be considered chaotic and scrambling. For our purposes, we will consider a system evolving under the *kicked-top* Hamiltonian. Following Ref. [37], we consider the Hamiltonian (setting $\hbar = 1$),

$$H = \frac{\kappa}{2j\tau} J_z^2 + pJ_y \sum_{n=-\infty}^{\infty} \delta\left(\frac{t}{\tau} - n_k\right). \quad (1)$$

In Eq. (1), τ represents the duration between periodic kicks (as indicated by the presence of the Dirac delta function), p is the strength of each kick (i.e. a turn by an angle p by each kick), κ is the (dimensionless) strength of the twist and ω_0 is the frequency constant. The twists are represented by the J_z^2 term whereas turns are associated with the J_y term. Additionally, the operators

J_α , $\alpha \in \{x, y, z\}$ denote collective spin operators. These operators can be chosen to describe a system of N spins such that if we represent the Pauli operators for the i -th spin by σ_α^i then

$$J_\alpha = \frac{1}{2} \sum_{i=1}^N \sigma_\alpha^i. \quad (2)$$

With the above definition the value j of the collective angular momentum satisfies $j = N/2$. Furthermore, we will use the following conventions

$$U_{\text{kick}} := \exp(-ipJ_y) \quad (3a)$$

$$U_{\text{twist}}(t) := \exp\left(-i\frac{\kappa}{2j\tau} J_z^2 t\right). \quad (3b)$$

In the calculations below we use the parameters $\kappa = 3.0$, $p = \pi/2$, and $\tau = 1.0$ since they allow us to study different kinds of behaviors in phase space [37]. Additionally, for our initial states, and to be as close to a classical state as possible, we will use the spin coherent states [38–40] given by

$$|\theta, \phi\rangle = \exp[(-i\theta(\sin(\phi)J_x - \cos(\phi)J_y))] |j, -j\rangle, \quad (4)$$

where $|j, -j\rangle$ represents the lowest value eigenstate of the J_z operator.

In order to sharpen our intuition, we first consider the case below the semiclassical limit. That is, in the limit in which $j \rightarrow \infty$, we define $X = \langle J_x \rangle / j$, $Y = \langle J_y \rangle / j$, and $Z = \langle J_z \rangle / j$. Under such conditions, it is possible to obtain the following equations of motion for the special case in which $p = \pi/2$ [41–45],

$$X((n+1)\tau) = Z(n\tau) \cos(\kappa X(n\tau)) + Y(n\tau) \sin(\kappa X(n\tau)), \quad (5a)$$

$$Y((n+1)\tau) = -Z(n\tau) \sin(\kappa X(n\tau)) + Y(n\tau) \cos(\kappa X(n\tau)), \quad (5b)$$

$$Z((n+1)\tau) = -X(n\tau) \quad (5c)$$

where $X(n)$, $Y(n)$, and $Z(n)$ denote the values of X , Y , and Z after n applications of the evolution operator $U_{\text{kick}} U_{\text{twist}}(\tau)$. In Fig. 1, we show a simple stroboscopic plot of the different initial coherent states that we use in our calculations and how they traverse the phase space for a total of $n_k = 50$ kicks. As we can appreciate in Fig. 1, as we get closer to the region of the phase space associated with chaos, the motion becomes more erratic and covers a wider section. This is shown by fixing θ_0 and choosing several initial conditions for ϕ_0 : for $\phi_0 = 0.63$ (circles), an elliptic fixed point is found; at $\phi_0 = 2.0$, there is a regular region (triangles), which reaches an edge at $\phi_0 = 1.05$, while for $\phi_0 = 2.0$ the system evolves in a sea of chaos.

In contrast to the semiclassical limit, when we study the purely quantum case, we can no longer describe states in phase space by points. Instead, we have to make use of distributions. While there are different possible distributions that can be used, for simplicity, we will use the

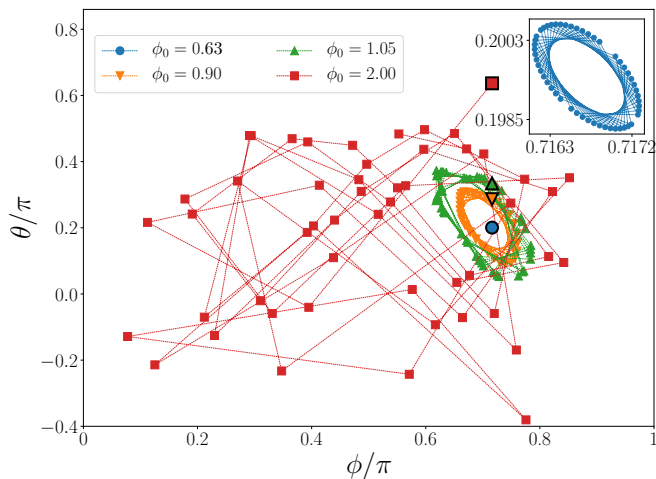


Figure 1. (Color online) Illustration of the dynamics of the classical kicked-top with $\kappa = 3.0$, $p = \pi/2$, and $\tau = 1.0$ for several initial conditions and $n_k = 50$ kicks. We use the following initial conditions: (a) *elliptic fixed point* with $\theta_0 = 2.25$, $\phi_0 = 0.63$, (b) *regular region point* with $\theta_0 = 2.25$, $\phi_0 = 0.90$, (c) *edge of chaos point* with $\theta_0 = 2.25$, $\phi_0 = 1.05$, and (d) *sea of chaos point* with $\theta_0 = 2.25$, $\phi_0 = 2.0$. The markers relative to the four points of phase space for the initial conditions are larger marker and have a black edge. Inset: the area of the elliptic fixed point is magnified.

Husimi Q function [46] to illustrate the behavior of the kicked-top in the quantum case. We define the Husimi Q function as

$$Q_\rho(\theta, \phi) := \langle \theta, \phi | \rho | \theta, \phi \rangle, \quad (6)$$

with ρ as the density matrix of the physical state of the system and $|\theta, \phi\rangle$ given by Eq. (4).

It is not difficult to see that for our choice of initial state, that is, a coherent state $|\theta_0, \phi_0\rangle$, its Q function is given by

$$Q_{|\theta_0, \phi_0\rangle}(\theta, \phi) = \left(\cos \frac{\Theta}{2} \right)^{4j}, \quad (7)$$

where Θ is the angle such that $\cos \Theta = \cos \theta \cos \theta_0 + \sin \theta \sin \theta_0 (\cos \phi \cos \phi_0 + \sin \phi \sin \phi_0)$. In other words, Θ is the angle between the vectors of the two points (θ, ϕ) and (θ_0, ϕ_0) on the unit sphere.

It is clear from Eq. (7) that as the number of spins increases, the distribution of our initial state becomes narrower. We illustrate this behavior in Fig. 2 for 5 spins (top row) and 100 spins (bottom row), respectively, using the same initial points in the phase space as those shown in Fig. 1.

When the system size is only a few spins (panels (a)-(d) of Fig. 2), the coherent states covers a wider section of phase space, and hence, after the dynamics, they have a non-negligible overlap. However, as the system size is increased (panels (e)-(h) of Fig. 2), the distribution of the state in phase space becomes narrower and the

choice of initial state matters: Only those initial states in the chaotic region of the semiclassical limit experience a behavior that smears their distribution across a large section of phase space (panel (h) in Fig. 2).

In our study of scrambling in the quantum kicked-top, we use the same parameters as in the semiclassical case and explore different diagnostics of scrambling. Below, we describe them in more detail.

III. MEASURES OF QUANTUM CHAOS

A. Out-of-time-ordered correlators and quantum chaos

Classically, we understand chaos as the exponential sensitivity to perturbations to initial conditions. We can express such a sensitivity with the aid of a Poisson bracket as

$$\{x(t), p(0)\}_{PB} \sim e^{\lambda t}. \quad (8)$$

In quantum mechanics, we have observables that do not commute, and the dynamics of closed systems are unitary. Therefore, we extend the notion of sensitivity to initial perturbations as follows. Consider a system with initial state ρ and evolving unitarily by the dynamics generated by a Hamiltonian H . Moreover, in order to extend Eq. (8) into the quantum case, we also use two initially commuting operators W and V . With these ingredients, we define the following

$$C(t) := \langle [W(t), V(0)]^\dagger [W(t), V(0)] \rangle. \quad (9)$$

In principle, for a system with a chaotic semiclassical limit we expect $C(t) \sim e^{2\lambda t}$. Here, $W(t) = U^\dagger W U$, and $U = \exp(iHt)$. At $t = 0$, $C(t)$ will be zero since the operators W and V initially commute. As the operators cease to commute because of the dynamics, the value of $C(t)$ will increase. If the dynamics and the initial state have no chaotic equivalent in the semiclassical limit, then the recurrence time for $C(t)$ will be comparatively small, and it will show revivals. However, for an appropriate initial state and Hamiltonian, there will be a persistent growth of $C(t)$ until it reaches a maximum value around which it will fluctuate.

We can also understand the dynamics by using the *out-of-time-ordered correlator*. It is given by

$$F(t) := \langle W^\dagger(t) V^\dagger W(t) V \rangle = \text{Tr} (W^\dagger(t) V^\dagger W(t) V \rho). \quad (10)$$

In the special case in which W and V are unitary operators, it is straightforward to verify that

$$C(t) = 2(1 - \text{Re}(F(t))). \quad (11)$$

Using a similar analysis to the one we did with $C(t)$, we can see that qualitatively, it is the persistent smallness of $F(t)$ that indicates we are observing chaotic behavior.

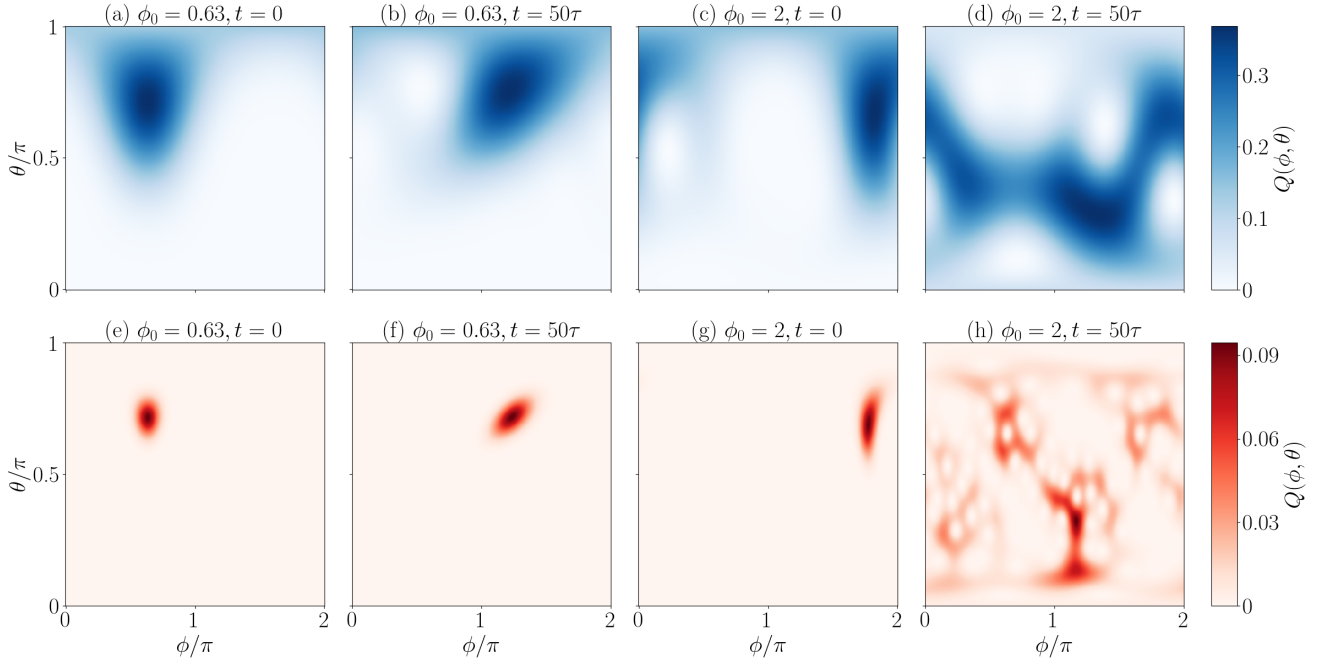


Figure 2. (Color online) Contour plot of the Husimi function $Q(\theta, \phi)$ for a system evolving under the Hamiltonian of Eq. (1), with $\kappa = 3.0$, $p = \pi/2$, and $\tau = 1.0$. Two systems are considered, $N = 5$ spins (top row) and $N = 100$ spins (bottom row), for which $t = 0$ is shown in panels (a), (c), (e), (g), and at time $t = 50\tau$, in panels (b), (d), (f), (h), for two initial conditions – $\theta_0 = 2.25$, $\phi_0 = 0.63$ and $\theta_0 = 2.25$, $\phi_0 = 2$, corresponding to the elliptic fixed point and the sea of chaos in Fig. 1.

In the case of the kicked-top, we use the operators

$$V = W(0) = \exp\left(\frac{1}{\sqrt{2j}}J_y\right). \quad (12)$$

With this choice, and initial coherent states as given by (4), we would expect that for initial states in the chaotic region and a sufficiently large system size, the OTOC would exhibit persistent smallness but otherwise exhibit quasiperiodic revivals. We will however further explore this behavior with the aid of quasiprobabilities related to OTOCs.

B. The nonclassicality behind OTOC's quasiprobabilities

In order to help identify relevant features of the dynamics of the kicked-top it is useful to expand the operators $W(t)$ and V in terms of the projectors onto their eigenspaces. When doing so, we can rewrite the OTOC as an expectation value of the product of eigenvalues, v_i, w_j , and obtain

$$F(t) = \sum_{v_1, w_2, v_2, w_3} v_1 w_2 v_2^* w_3^* \tilde{p}_t(v_1, w_2, v_2, w_3). \quad (13)$$

In the above,

$$\tilde{p}_t(v_1, w_2, v_2, w_3) := \text{Tr}\left(\Pi_{w_3}^{W(t)} \Pi_{v_2}^V \Pi_{w_2}^{W(t)} \Pi_{v_1}^V \rho\right). \quad (14)$$

We call this quantity the (coarse-grained) quasiprobability behind the OTOC. From previous work [35] we define the *cumulative nonclassicality* of the OTOC quasiprobability distribution,

$$\tilde{N}(t) := \sum_{v_1, w_2, v_2, w_3} |\tilde{p}_t(v_1, w_2, v_2, w_3)| - 1, \quad (15)$$

useful for detecting aspects of the dynamics that cannot be explained classically.

For the kicked-top model, we expect that initial states in the chaotic region will exhibit more nonclassicality after the unitary evolution generated by the Hamiltonian since we expect such states to be highly entangled.

C. Tripartite Mutual Information

As done in Ref. [17], it is possible to consider unitary channels acting on N qubit systems as states in a doubled Hilbert space and use the tripartite mutual information (TMI) involving partitions of the input and output spaces as a measure of scrambling. If a unitary $U(t)$ is defined in the product basis by

$$U(t) = \sum_{m=1}^{2^N} \sum_{m'=1}^{2^N} u_{m,m'} |m\rangle \langle m'| \quad (16)$$

then it is possible to also represent this as a $2N$ -qubit state by taking the tensor product of both the input and

output spaces of the channel

$$|U(t)\rangle = \frac{1}{2^{N/2}} \sum_{m=1}^{2^N} \sum_{m'=1}^{2^N} u_{m',m} |m\rangle_{in} \otimes |m'\rangle_{out}. \quad (17)$$

In particular, the identity channel can be written as

$$|\mathbb{I}\rangle = \frac{1}{2^{N/2}} \sum_{m=1}^{2^N} |m\rangle_{in} \otimes |m\rangle_{out}. \quad (18)$$

Hence, it is possible to rewrite Eq. (17) as

$$|U(t)\rangle = \mathbb{I} \otimes U(t) |\mathbb{I}\rangle. \quad (19)$$

Using the mapping between unitaries and states, we can then partition the input into subsystems A and B and the output into subsystems C and D and define the tripartite mutual information for a channel as

$$I_3(A : C : D) := I(A : C) + I(A : D) - I(A : CD). \quad (20)$$

The bipartite information between two subsystems, e.g. $I(A : C)$, is given by $I(A : C) = S_A + S_C - S_{AC}$. Here, each of the entropies requires the computation of a particular reduced density matrix. For instance, $S_{AC} = -\text{Tr}(\rho_{AC} \log_2 \rho_{AC})$ requires the calculation of $\rho_{AC} = \text{Tr}_{BD} \rho$. Here, ρ is the density matrix $|U(t)\rangle \langle U(t)|$ associated with the channel. Using the entanglement entropies we can rewrite Eq. (20) as

$$I_3(A : C : D) = S_A + S_C + S_D - S_{AC} - S_{AD} - S_{CD} + S_{ACD}. \quad (21)$$

While it is more common to calculate the TMI of a state of the system after the unitary evolution (as done for several many-body states in Refs. [24, 47]), the main motivation behind using the TMI of the state equivalent to the unitary evolution is that, channels that scramble will convert input states into locally indistinguishable output states. That is to say, the negativity of the tripartite mutual information in Eq. (20) signals multipartite entanglement between the input A and the output spaces C and D , and hence, channels that scramble will have a persistent negativity close to maximal.

In our calculations of the TMI for the kicked-top model, we will use the partition: A as one input spin, B $N-1$ as remaining input spins, C as one output spin, and D as $N-1$ remaining output spins. Interestingly, with this partition our tripartite mutual information calculations simplify since $S_A = 1$, $S_C = 1$, $S_D = 1$, $S_{CD} = N$, and $S_{ACD} = N-1$. Therefore, only S_{AC} and S_{AD} will have nontrivial contributions to I_3 of the kicked-top unitary channel.

IV. NUMERICAL SIMULATION RESULTS AND DISCUSSION

Here we calculate different measures of scrambling and nonclassicality as a function of time for initial states cor-

responding to the different initial points of the semiclassical phase space of Fig. 1.

Taking advantage of the permutational symmetry of the problem, we make use of the numerical libraries in [48] as implemented in [49, 50] to calculate the OTOC and the nonclassicality of its quasi-probability distribution using the Dicke basis. The benefit of this approach is that it is possible to obtain results even for larger system sizes (like $N = 100$) that would otherwise be too challenging to compute. We explain the details of the simulation in appendix A, and present our results in Figs. 3 and 8.

In Figs. 3 to 4 we can appreciate the real part of the OTOC and its power spectra for two different system sizes: $N = 5$ and $N = 100$. The power spectra of panel (b) are calculated simply with a discrete Fourier transform from the time-domain numerical data of panel (a). As is clear from the figures, in the case of the smaller system size, regardless of the initial state, it is not possible to observe a substantial difference between the different regions in phase space: both the real part of the OTOC and its power spectrum show no initial state dependence. As the system size is increased, the difference between the choice of initial state becomes more evident: The real part of the OTOC slowly decreases for all initial points. The peaks in the nonclassicality, corresponding to the kicks in the Hamiltonian, keep a hierarchy of the phase space points relation to chaos: the elliptic fixed point [$\phi/\pi = 0.63$ (blue curves)] is greater than the regular region [$\phi/\pi = 0.90$ (orange curves)], which is greater than the point at the edge of the sea of chaos [$\phi/\pi = 1.05$ (green curves)], which is greater than the point in the sea of chaos [$\phi/\pi = 2.0$ (red curves)].

In the nonclassicality in Figs. 5 and 6 for small systems, the difference between the behavior of the various initial states is difficult to distinguish. However, for a large system size the nonclassicality for the initial chaotic points has a slow onset towards a value around which it will later oscillate. This value is larger than the corresponding ones for the other initial states. Additionally, we also observe the effect that the system size has on the power spectra of the OTOC and the nonclassicality of its quasi-probability distribution – in all cases a $1/f$ noise type of behavior is observed.

For large system sizes and initial states in the chaotic sea, the kick harmonics are suppressed and there is an increased noise floor. This is to be expected of chaotic behavior that erases any signature of periodicity from the Hamiltonian. However, unlike the power spectra of the OTOC, the power spectra of the nonclassicality show little difference between the choice of initial state.

We now contrast the behavior of the OTOC, the nonclassicality of its quasiprobability distribution, and their power spectra with that of the entropy of entanglement for the reduced density matrix of one spin. In the case of the kicked-top there is evidence [42–44, 51–53] that indeed, the entanglement between one spin and the rest should have a similar behavior to what we have seen in the OTOC. We observe in Fig. 7 that as we make the sys-

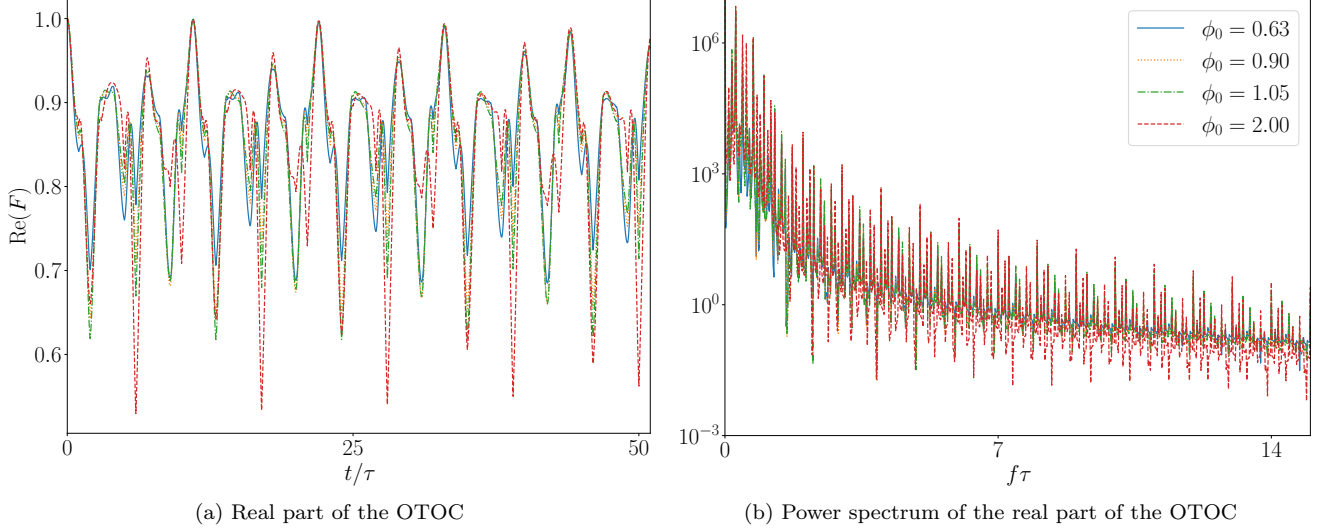


Figure 3. (Color online) $\text{Re}(F(t))$ and its power spectrum for a quantum kicked-top with $N = 5$ spins and $\kappa = 3.0$, $p = \pi/2$, and $\tau = 1.0$ for several initial conditions and $n_k = 50$ kicks. We use the following initial coherent states $|\theta_0, \phi_0\rangle$: (a) *elliptic fixed point* with $\theta_0 = 2.25$, $\phi_0 = 0.63$, (b) *regular region point* with $\theta_0 = 2.25$, $\phi_0 = 0.90$, (c) *edge of chaos point* with $\theta_0 = 2.25$, $\phi_0 = 1.05$, and (d) *sea of chaos point* with $\theta_0 = 2.25$, $\phi_0 = 2.0$.

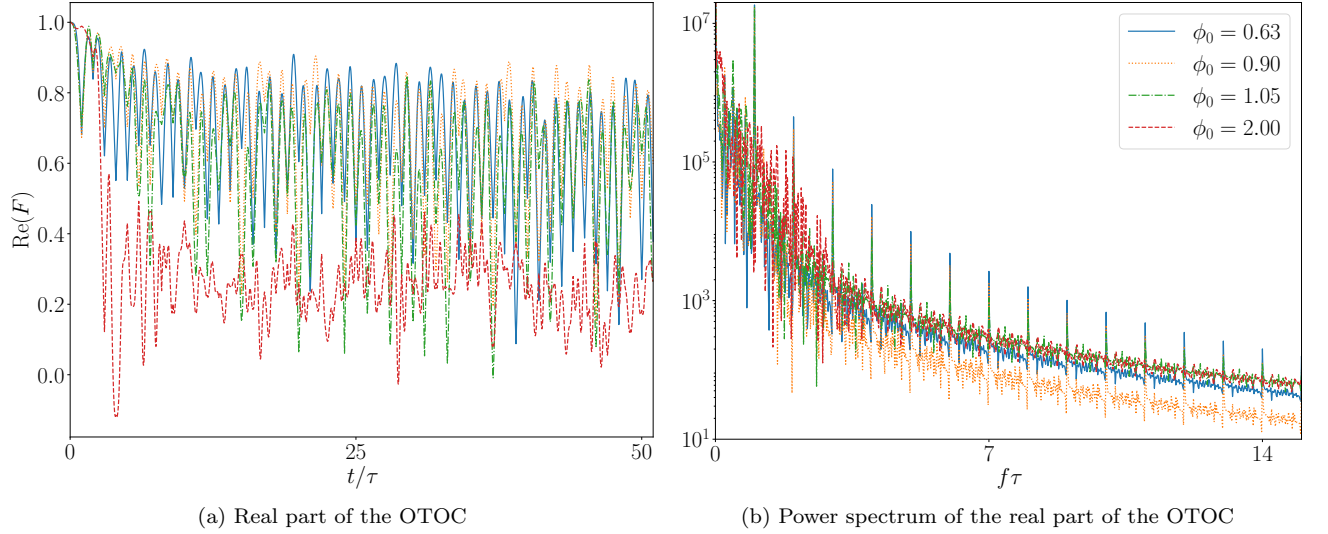


Figure 4. (Color online) $\text{Re}(F(t))$ and its power spectrum for a quantum kicked-top with $N = 100$ spins and $\kappa = 3.0$, $p = \pi/2$, and $\tau = 1.0$ for several initial conditions and $n_k = 50$ kicks. We use the following initial coherent states $|\theta_0, \phi_0\rangle$: (a) $\theta_0 = 2.25$, $\phi_0 = 0.63$, (b) $\theta_0 = 2.25$, $\phi_0 = 0.90$, (c) $\theta_0 = 2.25$, $\phi_0 = 1.05$, and (d) $\theta_0 = 2.25$, $\phi_0 = 2.0$.

tem size larger the difference between the initial states becomes more obvious, with the entanglement between one spin and the rest for the system with $N = 100$ spins being the largest when the initial state is in the sea of chaos. Furthermore, for an initial state in the chaotic region, we can also appreciate how by increasing the system size, the quasiperiodic oscillations in the entanglement entropy are also inhibited.

Finally, the results we obtain for the TMI of the channel offer similar conclusions to those of the OTOC, the

nonclassicality of its quasi-probability distribution, and the entanglement entropy of the reduced density matrix of one qubit regarding the effects of the size of the system. In Fig. 8 we can observe the TMI as well as the different entropies (and bipartite measures of mutual information) for the $N = 5$ case. The persistent negativity of the TMI signals a scrambling channel. However, we can also appreciate the effects of a small system size in the large fluctuations of the $I_3(A : C : D)$ and S_{AC} , $I(A : C)$, and $I(A : D)$. As the system grow larger, such

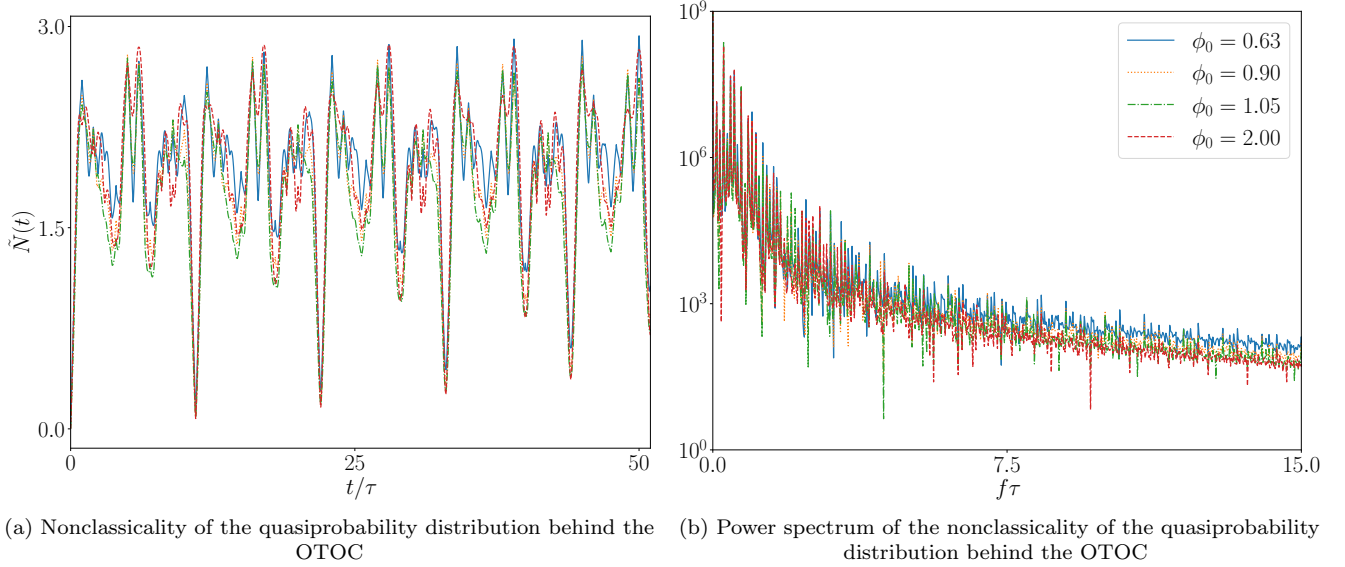


Figure 5. (Color online) Nonclassicality of the quasiprobability behind the OTOC and its power spectrum for a quantum kicked-top with $N = 5$ spins and $\kappa = 3.0$, $p = \pi/2$, and $\tau = 1.0$ for several initial conditions and $n_k = 50$ kicks. We use the following initial coherent states $|\theta_0, \phi_0\rangle$: (a) $\theta_0 = 2.25$, $\phi_0 = 0.63$, (b) $\theta_0 = 2.25$, $\phi_0 = 0.90$, (c) $\theta_0 = 2.25$, $\phi_0 = 1.05$, and (d) $\theta_0 = 2.25$, $\phi_0 = 2.0$.

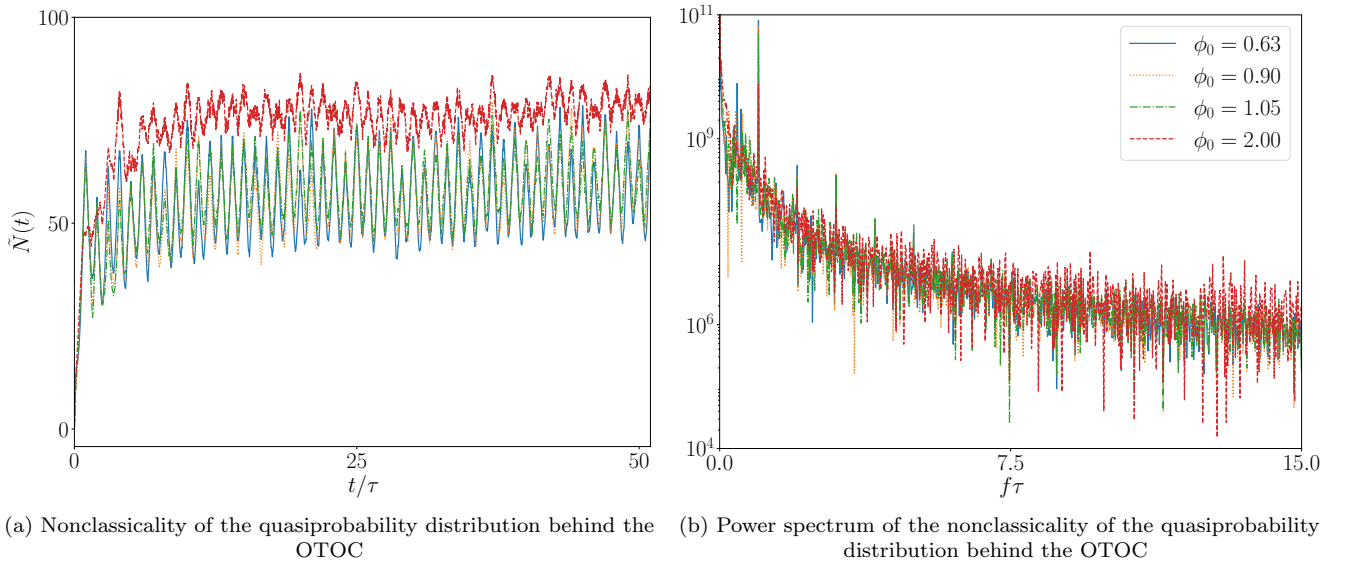


Figure 6. (Color online) Nonclassicality and its power spectrum for a quantum kicked-top with $N = 100$ spins and $\kappa = 3.0$, $p = \pi/2$, and $\tau = 1.0$ for several initial conditions and $n_k = 50$ kicks. We use the following initial coherent states $|\theta_0, \phi_0\rangle$: (a) $\theta_0 = 2.25$, $\phi_0 = 0.63$, (b) $\theta_0 = 2.25$, $\phi_0 = 0.90$, (c) $\theta_0 = 2.25$, $\phi_0 = 1.05$, and (d) $\theta_0 = 2.25$, $\phi_0 = 2.0$.

fluctuations are suppressed and the TMI gets closer to its lowest negative value.

Typically, scrambling is studied in the context of systems with a notion of spatial locality. In such a case, under unitary time evolution generated by an appropriate Hamiltonian H , initially local operators evolve into sums of products involving many high weight terms, that is, many operators acting on a high number of sites in

the system. However, such an intuition is not adequate for systems, such as the kicked-top, where the operators of interest act collectively. From our discussion of the kicked-top model in Sec. II, we can see then that scrambling is understood using phase space as follows: Operators and states that have distributions in phase space that are initially local are then smeared by the unitary chaotic evolution across a wide section of phase space

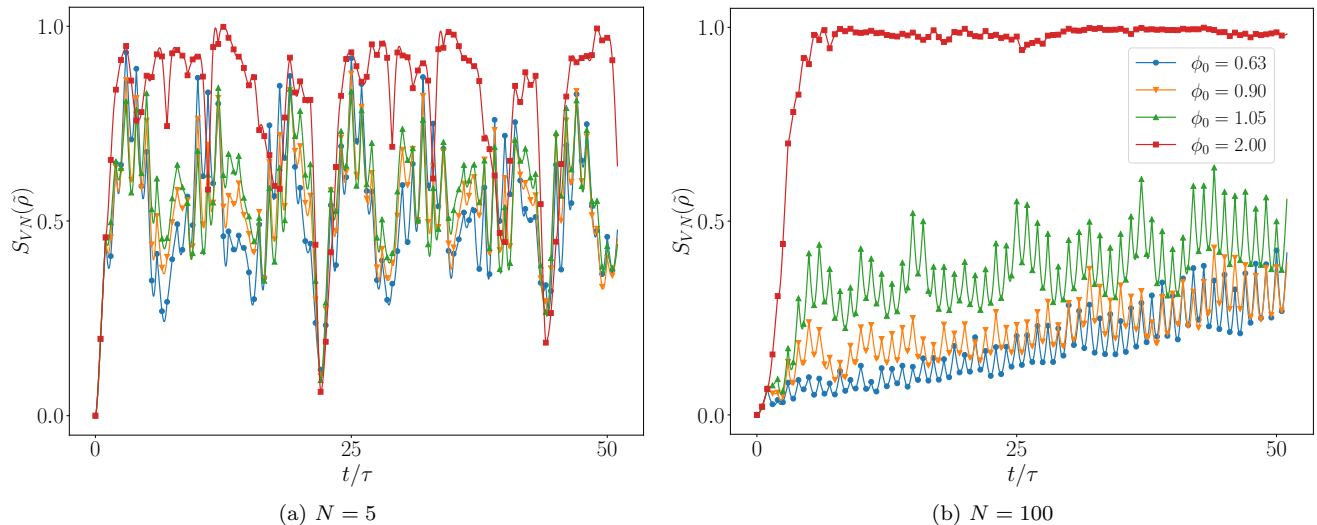


Figure 7. (Color online) Von Neumann entanglement entropy for the reduced density matrix of one spin in the kicked-top after evolving for a time t . Shown is the behavior with $\kappa = 3.0$, $p = \pi/2$, $\tau = 1.0$. Different initial spin coherent states $|\theta_0, \phi_0\rangle$ have the same value of $\theta_0 = 2.25$. By varying the value of ϕ_0 different types of behavior can be studied going from a point in the regular region of phase space ($\phi_0 = 0.63$) to a point in the sea of chaos ($\phi_0 = 2.0$). While the entanglement entropy is largest for the initial state in the sea of chaos, it is only after making the system size large that the difference between initial states becomes clear. Furthermore, in the chaotic case for a large N the signatures of the periodic nature of the Hamiltonian are lessened and it remains close to its theoretical maximal value.

with a long recurrence time. This explains both the persistent smallness of the OTOC and the TMI: as states and operators become less local in phase space then the square of their commutators with a fixed operator grows larger.

Additionally, we also see how the size of the system affects the entanglement entropy of the reduced density matrix of one spin. As was previously observed in [44], the entanglement of the $1 : N - 1$ partition depends on both the dimensions of the space and how close the dynamics leave a state to a spin coherent state. This explains why we observe higher entanglement, and thus a higher nonclassicality, for states in the chaotic region - the dynamics takes them away from spin coherent states.

V. CONCLUSIONS AND OUTLOOK

We see that the notion of scrambling as measured by the OTOC, the nonclassicality of its quasi-probability distribution, the TMI of the channel, or the entanglement entropy of the $1 : N - 1$ partition are all affected by the system size. When the system size is small, regardless of the measure used, the results can be misleading. In the case of the OTOC, the nonclassicality of its quasi-probability distribution, and the entanglement entropy we observe that for small system sizes the initial state makes little difference in the observed behavior.

Additionally, we can appreciate that all of these measures still exhibit quasiperiodic behavior even for initial states in the sea of chaos. In the case of the TMI, we

also observe fluctuations that are reminiscent of the periodic nature of the Hamiltonian. However, as the system size increases, the OTOC, the nonclassicality of its quasi-probability distribution, and the entanglement entropy all clearly show signatures of scrambling behavior only for initial states in the sea of chaos of the semiclassical limit of phase space.

Furthermore, for such states the fluctuations due to the periodic nature of the Hamiltonian are attenuated. We understand this behavior as being related to the delocalization of states in phase space. As the system size increases, the volume of phase space occupied by the initial states is smaller, and the dynamics will only smear the state across a large section of the phase space when the initial state is in the sea of chaos. Conversely, when the system size is small, most initial states will cover a wide section of the phase space, and the dynamics spreads the states in a very similar fashion. Thus, we can have a rather intuitive understanding of scrambling dynamics even in systems that lack a notion of spatial locality: scrambling is the delocalization of states in phase space.

Additionally, our comparison of the different tools to diagnose scrambling and quantum chaos highlights that while the channel TMI may start to signal scrambling at smaller system sizes than the OTOC, the nonclassicality of its quasi-probability distribution, or the entanglement entropy of the $1 : N - 1$ partition, it is also the most difficult to compute: it requires doubling the size of our space, and even in systems with a high degree of symmetry, this makes its computation challenging.

On the other hand, while the entanglement entropy of

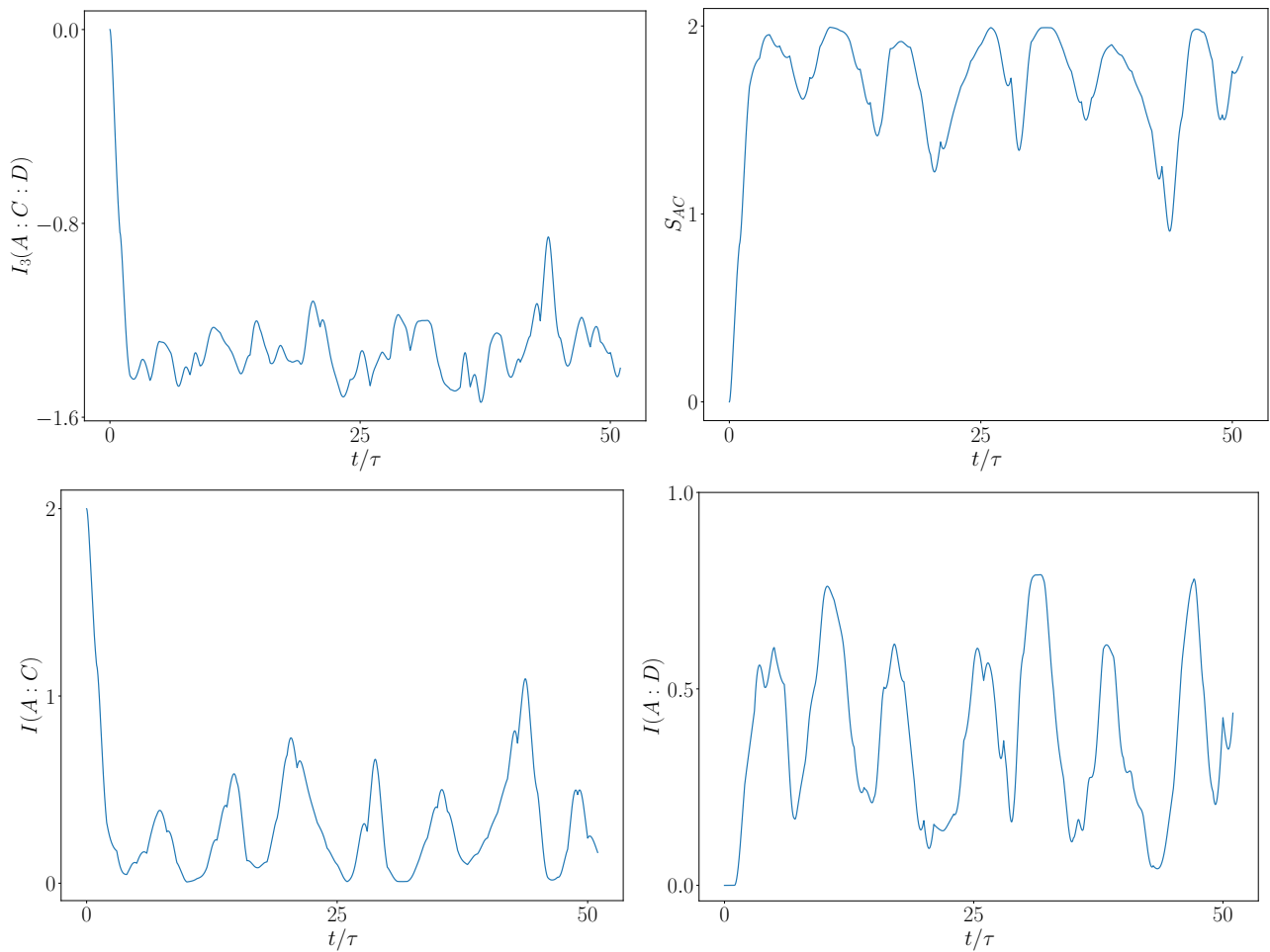


Figure 8. (Color online) Analysis of chaos and scrambling in the quantum kicked-top with $\kappa = 3.0$, $p = \pi/2$, $\tau = 1.0$, and $N = 5$ for the $1 : N - 1$ partition for both input and output of the unitary channel generated by the Hamiltonian. Given our choice of partition, I_3 is a trivial function of S_{AC} and S_{AD} . We appreciate in (a) that the tripartite mutual information I_3 shows persistent negativity with fluctuations that depend on the size of the system, and in (b) that S_{AC} oscillates quasi-periodically below its maximum value. We see also a conservation of information from the plots of the mutual information between subsystems A and C (in subplot(c)) and A and D (in subplot(d)). Whenever $I(A : C)$ reaches a maximum, $I(A : D)$ is at a minimum and vice versa. The oscillations present in all plots are due to the periodic nature of the Hamiltonian and they disappear as N becomes larger.

the $1 : N - 1$ partition might be the easiest to calculate, it would be the most affected by imperfections in an experimental setting. The calculation of the OTOC and the nonclassicality can be made efficiently by using the symmetries of the problem. Additionally, the nonclassicality is more robust than the OTOC, or the entanglement entropy, in the presence of experimental imperfections [54].

Our study highlights some future research opportunities. We have seen that the power spectrum of the OTOC and thenonclassicality of its quasi-probability distribution exhibit fluctuations that are attenuated at larger system sizes and for states in the chaotic region of phase space. So far the behaviors of these fluctuations have been studied for initial thermal states [55, 56]. However, it should be possible to do so for more general initial states - the size of such fluctuations could be used to di-

agnose quantum chaos. Additionally, while we did not compute it, it would be interesting to study the quasi-probability distribution of the kicked-top model system and verify whether a branching behavior similar to the one observed in spin chains is also observed.

Our work complements previous work on the fluctuation-dissipation theorem [55, 56], which illustrated a relation between chaotic dynamics in quantum systems and a nonlinear-response function in the OTOC. We further investigated the relation between the creation of entanglement and chaos in the quantum kicked-top, where in the comparison with the classical model provided by coherent spin states an upper bound for the Von Neumann entropy had been derived [44, 53].

Future work extending the current spin-system, finite-space analysis to the continuous-variable case through a

phase-space analysis may investigate those systems' different scrambling domains in different modes [57]. Additionally, another system that could be studied with the tools presented here is the family of kicked spin models in [58]. An interesting opportunity would be to apply the current analysis to light-matter models, where long-range interactions can be mediated by a common field, such as in the Dicke model [34, 59, 60]. Another interesting extension would be to analyze the scrambling behavior of the kicked top using temporal quantum steering [61]. We leave such an analysis for future work.

ACKNOWLEDGMENTS

JRGA wishes to thank Arjendu Pattanayak for helpful discussions. JRGA was supported by a fellowship from the Grand Challenges Initiative at Chapman University.

JD was partially supported by the Army Research Office (ARO) grant No. W911NF-18-1-0178. F.N. is supported in part by: Nippon Telegraph and Telephone Corporation (NTT) Research, the Japan Science and Technology Agency (JST) [via the Quantum Leap Flagship Program (Q-LEAP), the Moonshot R&D Grant Number JPMJMS2061, and the Centers of Research Excellence in Science and Technology (CREST) Grant No. JPMJCR1676], the Japan Society for the Promotion of Science (JSPS) [via the Grants-in-Aid for Scientific Research (KAKENHI) Grant No. JP20H00134 and the JSPS-RFBR Grant No. JPJSBP120194828], the Army Research Office (ARO) (Grant No. W911NF-18-1-0358), the Asian Office of Aerospace Research and Development (AOARD) (via Grant No. FA2386-20-1-4069), and the Foundational Questions Institute Fund (FQXi) via Grant No. FQXi-IAF19-06.

Appendix A: Efficient Numerical Simulation of the OTOC's quasi-probability distribution nonclassicality

The collective nonclassicality as defined by Eq. (15) might, at first, seem too complex a calculation to attempt. We need to compute, for every value of t , $(N+1)^4$ different quasiprobability cases. However, it is possible to obtain \tilde{N} , in practice, in a time comparable to that of an OTOC calculation provided we make some simpli-

fying assumptions. Since we are interested in using spin coherent states $|\theta, \varphi\rangle$ as the initial state of our system, then the cumulative nonclassicality becomes

$$\tilde{N}(t) = \sum_{v_1, w_2, v_2, w_3} \left| \langle \theta, \varphi | \hat{U}_t^\dagger | w_3 \rangle \right| \left| \langle w_3 | \hat{U}_t | v_2 \rangle \right| \times \left| \langle v_2 | \hat{U}_t^\dagger | w_2 \rangle \right| \left| \langle w_2 | \hat{U}_t | v_1 \rangle \right| \left| \langle v_1 | \theta, \varphi \rangle \right| - 1 \quad (\text{A1})$$

We define the following

$$\vec{s} := [v|\theta, \varphi] \quad (\text{A2a})$$

$$\hat{M}_t := [\langle w | \hat{U}_t | v \rangle] \quad (\text{A2b})$$

$$\vec{s}_t^T := \langle \theta, \varphi | \hat{U}_t^\dagger | w \rangle = \vec{s}^T \hat{M}_t^T \quad (\text{A2c})$$

With these simplifications the cumulative nonclassicality of the quasiprobability behind the OTOC's quasiprobability distribution can be written as

$$\tilde{N}(t) = |\vec{s}_t^T| |\hat{M}_t| |\hat{M}_t^T| |\hat{M}_t| |\vec{s}| - 1 \quad (\text{A3})$$

This suggests a straightforward procedure for calculating \tilde{N}

- Define dt as the length of the time step. Preallocate

$$\vec{s}, \hat{A} = \begin{bmatrix} \langle w | \\ \vdots \end{bmatrix}, \text{ and } \hat{B} = [|v\rangle \cdots]$$

- Define $U_t = \mathbb{I}$

- For each time step t :

- If a kick needs to be applied update the accumulation of unitaries as follows

$$U_t \leftarrow U_{\text{kick}} U_t \quad (\text{A4})$$

otherwise update with the twist term

$$U_t \leftarrow U_{\text{twist}}(dt) U_t \quad (\text{A5})$$

- Define $M_t = \hat{A} \hat{U}_t \hat{B}$.

- Compute $\vec{s}_t^T = \vec{s}^T \hat{M}_t^T$

- Store the cumulative nonclassicality at time t

$$\tilde{N}(t) = |\vec{s}_t^T| |\hat{M}_t| |\hat{M}_t^T| |\hat{M}_t| |\vec{s}| - 1 \quad (\text{A6})$$

[1] A. I. Larkin and Y. N. Ovchinnikov, “Quasiclassical Method in the Theory of Superconductivity,” *Soviet Journal of Experimental and Theoretical Physics* **28**, 1200 (1969).
[2] A. Kitaev, “Hidden correlations in the Hawking radiation and thermal noise,” (2014), talk given at Fundamental

Physics Prize Symposium.
[3] S. H. Shenker and D. Stanford, “Black holes and the butterfly effect,” *Journal of High Energy Physics* **2014** (2014), 10.1007/jhep03(2014)067.
[4] S. H. Shenker and D. Stanford, “Multiple shocks,” *Journal of High Energy Physics* **12**, 46 (2014),

- arXiv:1312.3296.
- [5] S. A. Hartnoll, “Theory of universal incoherent metallic transport,” *Nature Physics* **11**, 54 (2015), arXiv:1405.3651.
 - [6] S. H. Shenker and D. Stanford, “Stringy effects in scrambling,” *Journal of High Energy Physics* **5**, 132 (2015), arXiv:1412.6087.
 - [7] A. Kitaev, “A Simple Model of Quantum Holography,” (2015), KITP Strings Seminar and Entanglement.
 - [8] D. A. Roberts, D. Stanford, and L. Susskind, “Localized shocks,” *Journal of High Energy Physics* **2015** (2015), 10.1007/jhep03(2015)051.
 - [9] D. A. Roberts and D. Stanford, “Diagnosing Chaos Using Four-Point Functions in Two-Dimensional Conformal Field Theory,” *Physical Review Letters* **115**, 131603 (2015), arXiv:1412.5123.
 - [10] J. Maldacena, S. H. Shenker, and D. Stanford, “A bound on chaos,” *Journal of High Energy Physics* **8**, 106 (2016), arXiv:1503.01409.
 - [11] I. L. Aleiner, L. Faoro, and L. B. Ioffe, “Microscopic model of quantum butterfly effect: Out-of-time-order correlators and traveling combustion waves,” *Annals of Physics* **375**, 378 (2016), arXiv:1609.01251.
 - [12] M. Blake, “Universal Charge Diffusion and the Butterfly Effect in Holographic Theories,” *Physical Review Letters* **117**, 091601 (2016).
 - [13] M. Blake, “Universal diffusion in incoherent black holes,” *Physical Review D* **94**, 086014 (2016).
 - [14] Y. Chen, “Universal Logarithmic Scrambling in Many Body Localization,” ArXiv e-prints (2016), arXiv:1608.02765.
 - [15] A. Lucas and J. Steinberg, “Charge diffusion and the butterfly effect in striped holographic matter,” *Journal of High Energy Physics* **2016**, 143 (2016).
 - [16] D. A. Roberts and B. Swingle, “Lieb-Robinson Bound and the Butterfly Effect in Quantum Field Theories,” *Physical Review Letters* **117**, 091602 (2016).
 - [17] P. Hosur, X.-L. Qi, D. A. Roberts, and B. Yoshida, “Chaos in quantum channels,” *Journal of High Energy Physics* **2**, 4 (2016), arXiv:1511.04021.
 - [18] S. Banerjee and E. Altman, “Solvable model for a dynamical quantum phase transition from fast to slow scrambling,” *Physical Review B* **95** (2017), 10.1103/PhysRevB.95.134302.
 - [19] R. Fan, P. Zhang, H. Shen, and H. Zhai, “Out-of-time-order correlation for many-body localization,” *Science Bulletin* **62**, 707 (2017).
 - [20] Y. Gu, X.-L. Qi, and D. Stanford, “Local criticality, diffusion and chaos in generalized Sachdev-Ye-Kitaev models,” *Journal of High Energy Physics* **2017**, 125 (2017).
 - [21] D. A. Roberts and B. Yoshida, “Chaos and complexity by design,” *Journal of High Energy Physics* **4**, 121 (2017), arXiv:1610.04903.
 - [22] X. Chen and T. Zhou, “Operator scrambling and quantum chaos,” ArXiv e-prints (2018), arXiv:1804.08655.
 - [23] Y. Huang, Y.-L. Zhang, and X. Chen, “Out-of-time-ordered correlators in many-body localized systems,” *Annalen der Physik* **529**, 1600318 (2017), arXiv:1608.01091.
 - [24] E. Iyoda and T. Sagawa, “Scrambling of Quantum Information in Quantum Many-Body Systems,” *Physical Review A* **97**, 042330 (2018), arXiv:1704.04850.
 - [25] B. Yoshida and A. Kitaev, “Efficient decoding for the Hayden-Preskill protocol,” ArXiv e-prints (2017), arXiv:1710.03363.
 - [26] C.-J. Lin and O. I. Motrunich, “Out-of-time-ordered correlators in a quantum Ising chain,” *Physical Review B* **97**, 144304 (2018).
 - [27] S. Pappalardi, A. Russomanno, B. Žunković, F. Iemini, A. Silva, and R. Fazio, “Scrambling and entanglement spreading in long-range spin chains,” *Physical Review B* **98**, 134303 (2018), arXiv:1806.00022.
 - [28] N. Yunger Halpern, A. Bartolotta, and J. Pollack, “Entropic uncertainty relations for quantum information scrambling,” *Communications Physics* **2**, 1 (2019).
 - [29] B. Vermersch, A. Elben, L. M. Sieberer, N. Y. Yao, and P. Zoller, “Probing scrambling using statistical correlations between randomized measurements,” *Phys. Rev. X* **9**, 021061 (2019).
 - [30] A. W. Harrow, L. Kong, Z.-W. Liu, S. Mehraban, and P. W. Shor, “Separation of out-of-time-ordered correlation and entanglement,” *PRX Quantum* **2**, 020339 (2021).
 - [31] Z. Cao, Z. Xu, and A. del Campo, “Diagnosing quantum chaos in multipartite systems,” arXiv preprint arXiv:2111.12475 (2021), 2111.12475.
 - [32] J. Braumüller, A. H. Karamlou, Y. Yanay, B. Kannan, D. Kim, M. Kjaergaard, A. Melville, B. M. Niedzielski, Y. Sung, A. Vepsäläinen, R. Winik, J. L. Yoder, T. P. Orlando, S. Gustavsson, C. Tahan, and W. D. Oliver, “Probing quantum information propagation with out-of-time-ordered correlators,” *Nature Physics* (2021), 10.1038/s41567-021-01430-w.
 - [33] X. Mi, P. Roushan, C. Quintana, S. Mandrà, J. Marshall, C. Neill, F. Arute, K. Arya, J. Atalaya, R. Babbush, and et al., “Information scrambling in quantum circuits,” *Science* **374**, 1479–1483 (2021).
 - [34] A. Leroche and S. Pappalardi, “Bridging entanglement dynamics and chaos in semiclassical systems,” *Phys. Rev. A* **102**, 032404 (2020).
 - [35] J. R. González Alonso, N. Yunger Halpern, and J. Dreschel, “Out-of-Time-Ordered-Correlator Quasiprobabilities Robustly Witness Scrambling,” *Physical Review Letters* **122**, 040404 (2019).
 - [36] N. J. Cerf and C. Adami, “Information theory of quantum entanglement and measurement,” *Physica D: Nonlinear Phenomena* **120**, 62 (1998).
 - [37] X. Wang, S. Ghose, B. C. Sanders, and B. Hu, “Entanglement as a signature of quantum chaos,” *Physical Review E* **70**, 016217 (2004).
 - [38] P. W. Atkins and J. C. Dobson, “Angular Momentum Coherent States,” *Proceedings of the Royal Society of London. Series A, Mathematical and Physical Sciences* **321**, 321 (1971).
 - [39] F. T. Arecchi, E. Courtens, R. Gilmore, and H. Thomas, “Atomic Coherent States in Quantum Optics,” *Physical Review A* **6**, 2211 (1972).
 - [40] W.-M. Zhang, D. H. Feng, and R. Gilmore, “Coherent states: Theory and some applications,” *Reviews of Modern Physics* **62**, 867 (1990).
 - [41] F. Haake, M. Kuś, and R. Scharf, “Classical and quantum chaos for a kicked top,” *Zeitschrift für Physik B Condensed Matter* **65**, 381 (1987).
 - [42] S. Ghose, C. R. Paul, and R. Stock, “Quantum chaos and tunneling in the kicked top,” *Laser Physics* **18**, 1098 (2008).
 - [43] S. Ghose, R. Stock, P. Jessen, R. Lal, and A. Silberfarb, “Chaos, entanglement, and decoherence in the quantum kicked top,” *Physical Review A* **78** (2008), 10.1103/Phys-

- RevA.78.042318.
- [44] M. Kumari and S. Ghose, “Untangling entanglement and chaos,” *Physical Review A* **99**, 042311 (2019).
 - [45] F. Haake, *Quantum Signatures of Chaos* (Springer Berlin Heidelberg, 2001).
 - [46] K. Husimi, “Some Formal Properties of the Density Matrix,” *Proceedings of the Physico-Mathematical Society of Japan. 3rd Series* **22**, 264 (1940).
 - [47] A. Seshadri, V. Madhok, and A. Lakshminarayan, “Tripartite mutual information, entanglement, and scrambling in permutation symmetric systems with an application to quantum chaos,” *Physical Review E* **98**, 052205 (2018), [arXiv:1806.00113](#).
 - [48] N. Shammah, S. Ahmed, N. Lambert, S. De Liberato, and F. Nori, “Open quantum systems with local and collective incoherent processes: Efficient numerical simulation using permutational invariance,” *Physical Review A* **98** (2018), 10.1103/PhysRevA.98.063815, [arXiv:1805.05129](#).
 - [49] J. R. Johansson, P. D. Nation, and F. Nori, “QuTiP: An open-source Python framework for the dynamics of open quantum systems,” *Computer Physics Communications* **183**, 1760 (2012), [arXiv:1110.0573](#).
 - [50] J. R. Johansson, P. D. Nation, and F. Nori, “QuTiP 2: A Python framework for the dynamics of open quantum systems,” *Computer Physics Communications* **184**, 1234 (2013), [arXiv:1211.6518](#).
 - [51] C. Neill, P. Roushan, M. Fang, Y. Chen, M. Kolodrubetz, Z. Chen, A. Megrant, R. Barends, B. Campbell, B. Chiaro, A. Dunsworth, E. Jeffrey, J. Kelly, J. Mutus, P. J. J. O’Malley, C. Quintana, D. Sank, A. Vainsencher, J. Wenner, T. C. White, A. Polkovnikov, and J. M. Martinis, “Ergodic dynamics and thermalization in an isolated quantum system,” *Nature Physics* **12**, 1037 (2016).
 - [52] J. B. Ruebeck, J. Lin, and A. K. Pattanayak, “Entanglement and its relationship to classical dynamics,” *Physical Review E* **95**, 062222 (2017).
 - [53] M. Kumari and S. Ghose, “Quantum-classical correspondence in the vicinity of periodic orbits,” *Phys. Rev. E* **97**, 052209 (2018).
 - [54] N. Yunger Halpern, B. Swingle, and J. Dressel, “Quasiprobability Behind the Out-of-Time-Ordered Correlator,” *Physical Review A* **97**, 042105 (2018).
 - [55] N. Tsuji, T. Shitara, and M. Ueda, “Out-of-time-order fluctuation-dissipation theorem,” *Physical Review E* **97** (2018), 10.1103/PhysRevE.97.012101, [arXiv:1612.08781](#).
 - [56] N. Tsuji and M. Ueda, “Fluctuation theorem for quantum-state statistics,” [arXiv:1807.11683 \[cond-mat, physics:quant-ph\]](#) (2018), [arXiv:1807.11683 \[cond-mat, physics:quant-ph\]](#).
 - [57] Q. Zhuang, T. Schuster, B. Yoshida, and N. Y. Yao, “Scrambling and complexity in phase space,” *Physical Review A* **99**, 062334 (2019).
 - [58] M. H. Muñoz-Arias, P. M. Poggi, and I. H. Deutsch, “Nonlinear dynamics and quantum chaos of a family of kicked spin models,” *Physical Review E* **103**, 052212 (2021).
 - [59] A. Leroise and S. Pappalardi, “Origin of the slow growth of entanglement entropy in long-range interacting spin systems,” *Phys. Rev. Research* **2**, 012041 (2020).
 - [60] S. Sinha, S. Ray, and S. Sinha, “Fingerprint of chaos and quantum scars in kicked Dicke model: an out-of-time-order correlator study,” *Journal of Physics: Condensed Matter* **33**, 174005 (2021).
 - [61] J.-D. Lin, W.-Y. Lin, H.-Y. Ku, N. Lambert, Y.-N. Chen, and F. Nori, “Quantum steering as a witness of quantum scrambling,” *Phys. Rev. A* **104**, 022614 (2021).